

# Silicon Carbide Growth using Laser Chemical Vapor Deposition

Jian Mi, Josh Gillespie, Ryan W. Johnson, Scott N. Bondi, and W. Jack Lackey  
Rapid Prototyping and Manufacturing Institute  
Woodruff School of Mechanical Engineering  
Georgia Institute of Technology  
Atlanta, GA 30332-0405  
Reviewed, accepted August 13, 2003

## Abstract

Silicon Carbide (SiC) has been grown from methyltrichlorosilane (MTS) and hydrogen using the Georgia Tech Laser Chemical Vapor Deposition (LCVD) system. A morphology study of LCVD-SiC fibers and lines was completed. Graphite and single crystal silicon were used as the substrates. In order to provide guidance to future growth of SiC, thermodynamic calculations for the C-H-Si-Cl system were performed using the SOLGASMIX-PV program.

## Introduction

Silicon carbide (SiC) has outstanding material properties, including extreme hardness, high electrical breakdown field, wide band gap energy, good thermal conductivity, and excellent resistance to corrosion and thermal shock. It is either presently being used or considered primarily for use in critical parts for uncooled gas turbine and adiabatic diesel engines and high temperature bearings. It is also currently being considered for use in semiconductor devices, especially for high temperature, high frequency, and high power electronic applications.

Laser Chemical Vapor Deposition (LCVD) is a process that uses a laser to initiate a chemical reaction of gaseous reactants, which results in solid deposits on selectively heated areas of the substrate. The LCVD technique has the potential to make small and complex shaped metal and ceramic parts. Due to the nature of the LCVD process, deposited materials have desirable properties, such as purity and little porosity. There are very few papers on making SiC using LCVD. T. Noda *et al.*<sup>1</sup> reported the formation of polycrystalline SiC by excimer-laser chemical vapor deposition. Chin *et al.*<sup>2</sup> explored the relationship between the morphology and experimental parameters of CVD-SiC prepared from  $\text{CH}_3\text{SiCl}_3$  and  $\text{H}_2$ . Choi *et al.*<sup>3</sup> reported the CVD-SiC microstructure obtained from different chlorosilanes, such as DDS ( $((\text{CH}_3)_2\text{SiCl}_2)$ ), TCS ( $((\text{CH}_3)_3\text{SiCl}_2)$ ), and TS ( $((\text{CH}_3)_4\text{Si})$ ). Tsui *et al.*<sup>4</sup> tried to explain the observed morphology of CVD-SiC with chemical kinetics and mass transport arguments. In our research, SiC lines and fibers have been grown using the Georgia Tech LCVD system for the pyrolysis of  $\text{CH}_3\text{SiCl}_3$  (MTS, methyltrichlorosilane) and  $\text{H}_2$ . A morphological study of the SiC lines and fibers was performed, which gave indications of the LCVD-SiC growth mechanism.

Thermodynamic calculations are extremely useful for analyzing the combination of condensed phases that will be most stably deposited during the LCVD process.

Thermodynamic calculations based on making SiC from the C-H-Si-Cl system, which represents the experimental mixture of  $\text{CH}_3\text{SiCl}_3$  and  $\text{H}_2$ , were explored using the SOLGASMIX-PV computer program. The calculations are based on minimization of the Gibb's free energy of the system, which has been explained in detail by Eriksson.<sup>5</sup> Volcano effects<sup>6</sup> have been observed in the SiC fibers & lines produced by the Georgia Tech LCVD apparatus. Volcano effects are undesirable because of detrimental results for surface quality and component fabrication. Hopefully, the thermodynamic calculations will help to explain the cause of the volcano effects and offer direction how to avoid them.

## Experimental

Duty et al.<sup>7</sup> described the Georgia Tech LCVD system in detail. For the deposition of SiC, a vaporizer (bubbler) was used. A simple schematic drawing of vaporizing the liquid MTS and transporting the vapor MTS to the reaction chamber is shown in Figure 1. Normally, MTS is assumed saturated under room temperature. The amount of MTS flowing into the reaction chamber was controlled by the amount of input hydrogen at given temperature and pressure. In order to meet the desired dilution ratio of MTS to  $\text{H}_2$ , more  $\text{H}_2$  was introduced downstream of the vaporizer. For all the experiments, the pressure of the reaction chamber was maintained at 500 Torr. The growth temperature was measured and controlled by a thermal imager.<sup>7</sup> Process variables that were investigated were deposition temperature, reagent flow rate, and the MTS to  $\text{H}_2$  ratio.

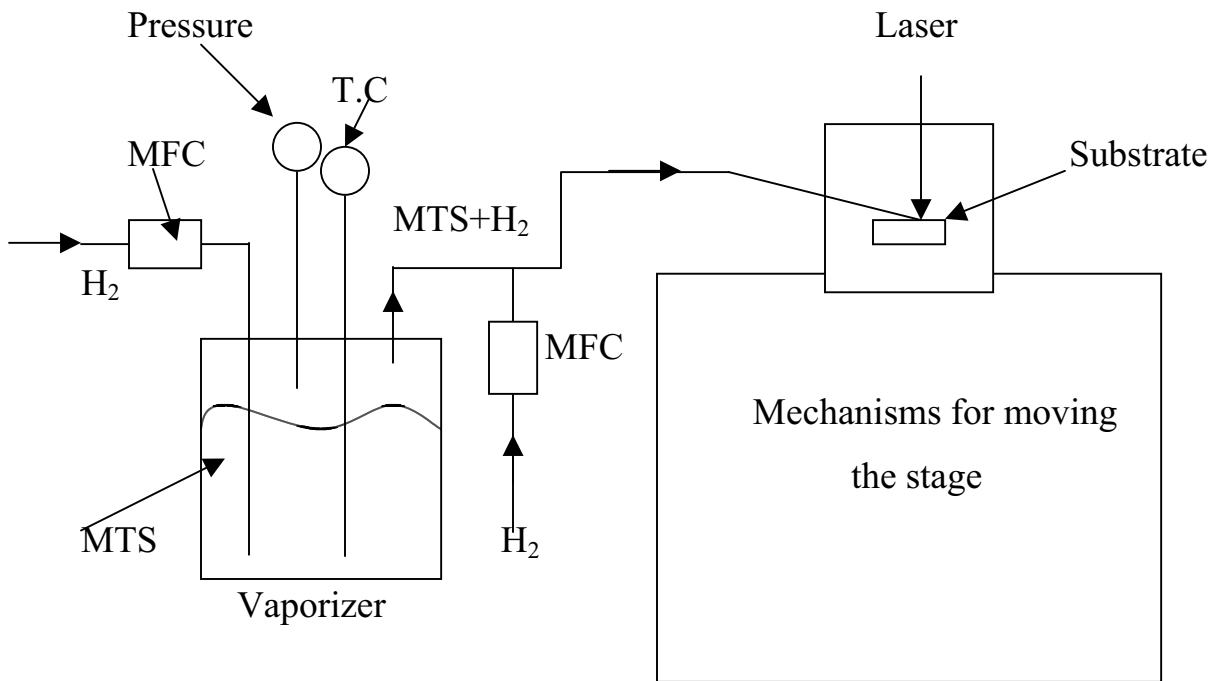


Figure 1 Reagent supply system

## LCVD-SiC

Fibers and lines of SiC were grown using the Georgia Tech LCVD system. The experimental variables for the SiC fibers and lines are shown in Tables 1 and 2. The SEM micrographs in Figures 2 - 6 show the deposit microstructure and permitted correlating the processing conditions with the microstructure. Many morphologies were observed. These include nodular, rounded columnar, strongly faceted, and needle like structures.

For the fibers of the L176 series of experiments (Figure 2), as temperature decreased, the surface morphology changed from strongly faceted to nodular. This may be explained by the fact that temperature often influences nucleation.<sup>8</sup> For the fibers with faceted surface structures, the outer regions of the fibers, which have lower growth temperatures than the middle region, nodular structures were commonly observed for almost all the LCVD-SiC fibers. Surprisingly, the grains in the center of the deposit were often smaller than at the outer region.

As the ratio of MTS to H<sub>2</sub> increased, the crystallite sizes were increased in the indicated deposition temperature range as can be seen in Figure 3. For CVD of SiC Tsui et al.<sup>4</sup> found that the change in concentration of MTS affected the surface structures to a lesser extent than the growth temperature. As shown in Figures 2 and 3, the fibers typically had larger crystallites at the outer regions than in the middle areas.

Except for L265-7 and L265-8 shown in Figure 4, all of the SiC fibers showed depressions in the middle. This is known as the volcano effects.<sup>6</sup> Depressions were present because of either high temperatures or the lack of reactants in the effected region. Future work is needed to understand the reasons and to determine how to grow SiC fibers without these defects.

The observed LCVD-SiC fiber morphologies did not correlate well with the relationships of CVD SiC morphology vs. process parameters described by Chin.<sup>2</sup> The reasons are, probably, that for the LCVD process, the temperatures within the reaction zone are not constant while during the CVD process the whole reaction region has the same temperature. As for the SiC fibers grown on single crystal Si, shown in Figure 5, they show similar morphology and bad volcano effects, but different from those grown on the graphite substrate.

Figure 6 shows LCVD-SiC lines grown on graphite and single crystal Si. The lines on graphite have nodular surface structures. Fine crystallites were obtained in the middle region and coarse crystallites were observed at the outer areas. This is consistent with the observation for fibers. The lines on single crystal Si show different morphologies from those on graphite. For the line on the smooth surface of the single crystal Si, there is more material in the middle. For the line on the rough surface of single crystal Si, the line is very flat.

The laser used to deposit SiC has a laser spot of 200  $\mu\text{m}$  in diameter on the substrate. But all the fibers grown are at least twice as big in diameter, which are shown in Table 3.

This indicates that the laser used to initiate the chemical reaction introduced a reaction zone much bigger than the spot size of the laser. For the processing conditions investigated, the spatial resolution for making SiC parts using the LCVD system is bigger than the laser spot size, which will require special attention for process and component modeling.

Table 1. Experimental variables of LCVD-SiC fibers

Sample No.	Substrate	Gas-jet	<sup>a</sup> Growth temp (°C)	Growth pressure (Torr)	H <sub>2</sub> flow (cm <sup>3</sup> /min)	MTS flow (cm <sup>3</sup> /min)	Volume ratio MTS:H <sub>2</sub>
L176-3	Graphite	Off	<sup>b</sup> N/A	500	500	25	1:20
L176-4	Graphite	Off	1600	500	500	25	1:20
L176-5	Graphite	Off	1600-1550	500	500	25	1:20
L176-6	Graphite	Off	<sup>c</sup> 1600	500	500	25	1:20
L265-1	Graphite	On	1300	500	500	5	1:100
L265-5	Graphite	On	1350	500	500	8.4	1:60
L265-7	Graphite	On	1300	500	500	25	1:20
L265-8	Graphite	On	1400	500	500	25	1:20
L252-2	<sup>d</sup> Single Si	On	977	500	500	5	1:100
L253-2	<sup>e</sup> Single Si	On	980-1011	500	500	5	1:100

<sup>a</sup> Temperature averaged over a given region

<sup>b</sup> Laser power higher than for other L176 experiments

<sup>c</sup> Temperature averaged over a smaller region than the one most commonly used, therefore, the actual temperature was lower than for L176-3 through L176-5

<sup>d</sup> Polished surface of Si wafer

<sup>e</sup> Rough surface of Si wafer

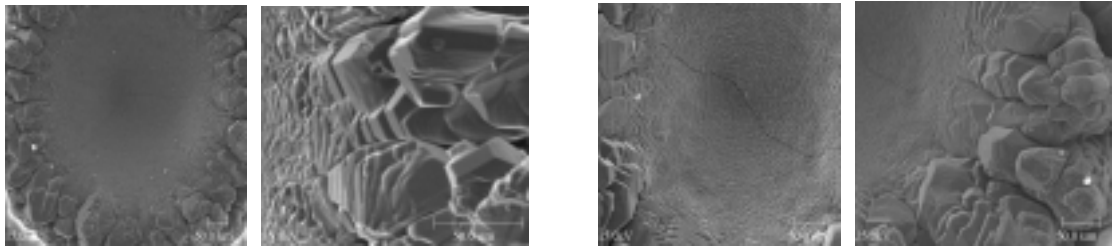
Table 2. Experimental variables of LCVD-SiC lines

Sample No.	Substrate	Gas-jet	<sup>a</sup> Growth temp (°C)	Growth pressure (Torr)	H <sub>2</sub> flow (cm <sup>3</sup> /min)	MTS flow (cm <sup>3</sup> /min)	Volume ratio MTS:H <sub>2</sub>
L251-1	Graphite	On	1265	500	500	25	1:20
L252-3	<sup>b</sup> Single Si	On	900-1000	500	500	5	1:100
L253-1	<sup>c</sup> Single Si	On	970	500	500	5	1:100

<sup>a</sup> Temperature averaged over a given region

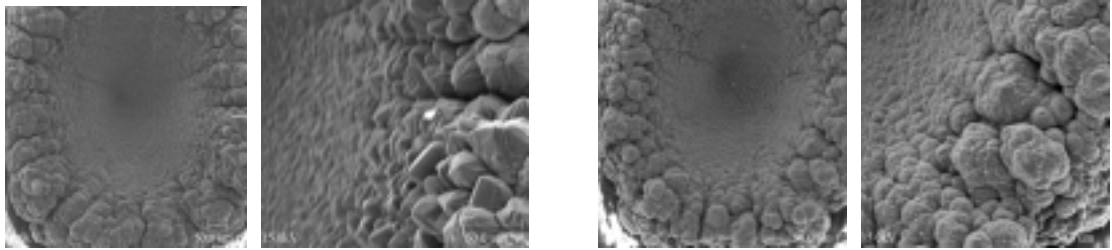
<sup>b</sup> Polished surface of Si wafer

<sup>c</sup> Rough surface of Si wafer



L 176-3

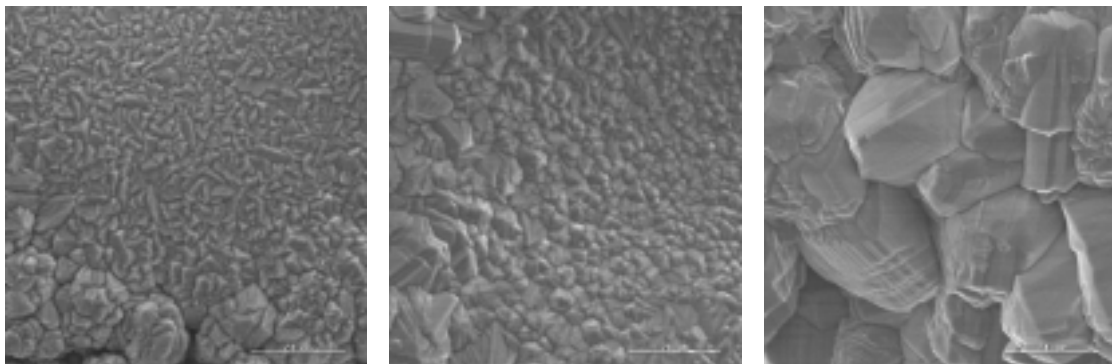
L176-4



L 176-5

L176-6

Figure 2 Microstructure of fibers in L176 series of experiments

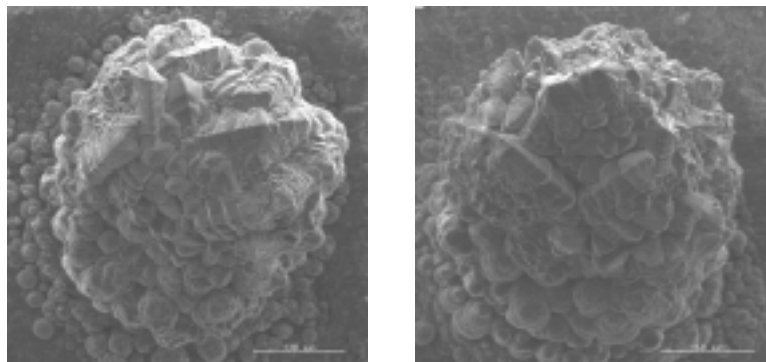


L 265-1

L 265-5

L265-7

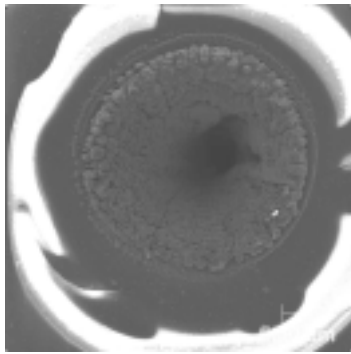
Figure 3 Influence of MTS to H2 ration on crystallite size



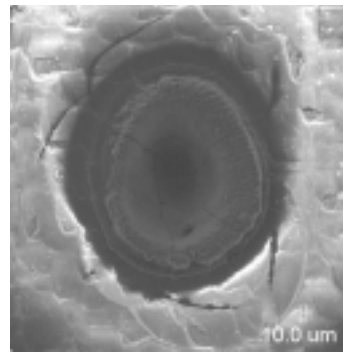
L 265-7

L265-8

Figure 4 SiC fibers without volcano effects

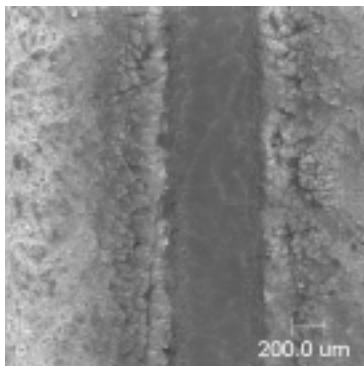


L252-2

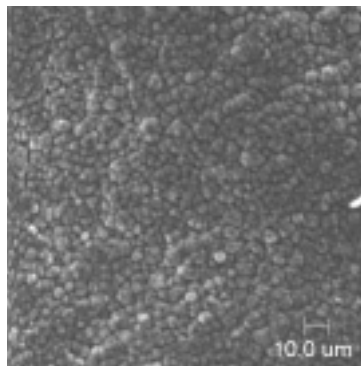


L253-2

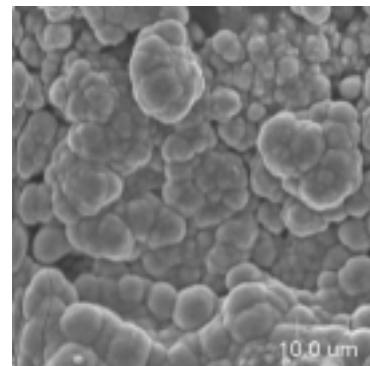
Figure 5 SiC fibers grown on single crystal Si



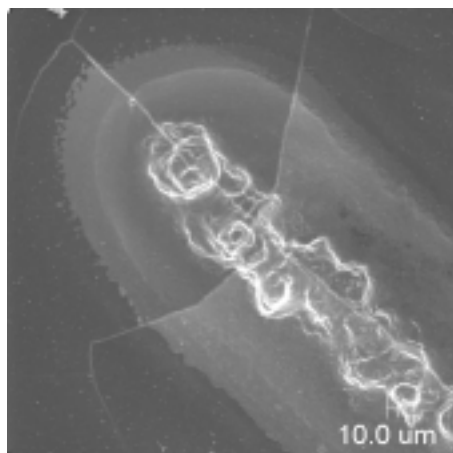
L251-1



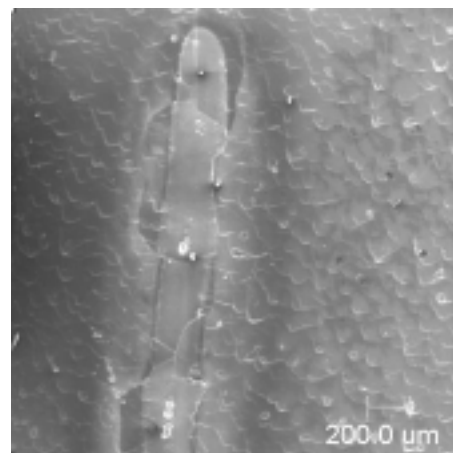
L251-1-middle



L251-1-outer



L252-3



L253-1

Figure 6 SiC lines on grown by LCVD

Table 3. Diameters of LCVD-SiC fibers

Sample No.	T <sub>avg</sub> (°C)	MTS: H <sub>2</sub>	<sup>a</sup> D <sub>inner</sub> (μm)	<sup>b</sup> D <sub>outer</sub> (μm)
L265-1	1300	1: 100	423.0	838.4
L265-2	1400	1: 100	510.1	947.2
L265-3	1250	1: 60	366.1	801.8
L265-5	1350	1: 60	479.8	841.9
L265-6	1450	1: 60	616.5	924.0
L265-7	1300	1: 20	621.4	788.3
L265-8	1400	1: 20	781.9	958.5

<sup>a</sup> Actual fiber size

<sup>b</sup> The whole region that has SiC deposited

### Thermodynamic Calculations

The C-H-Si-Cl system used to simulate the deposition of SiC was defined by specifying pressure, temperature, and the amount of each element present. By holding the pressure and temperature constant, the volume of the system can expand and contract during reaction depending on the given pressure and temperature. Because the calculations are based upon equilibrium thermodynamics, the final results are independent of the initial form of the elements. Therefore, while inputting the element mole value, the concern is the molecular ratios of each element to satisfy the initial gas reactants used. Also, it is assumed that the reactions in the gas phase come to equilibrium quickly, and the molecules formed represent the most stable distribution.

Two sets of thermodynamic calculations were performed; one was based on MTS and H<sub>2</sub>, which were used for growing SiC. The other set was based on the mixture of CCl<sub>4</sub>, SiCl<sub>4</sub>, and H<sub>2</sub>, which were used to check our calculations with those of Kingon et al.<sup>9</sup> The MTS set included 44 gas species and 5 condensed phases (graphite, liquid silicon, solid silicon, α-SiC, and β-SiC). Those species are listed in Table 4. For the calculations including CCl<sub>4</sub> and SiCl<sub>4</sub>, the species considered by Kingon were used<sup>8</sup>, which are shown in Table 5. The enthalpies of formation and entropies of formation were taken from the JANAF Thermodynamical Tables.<sup>10</sup>

Table 4. Species considered in the C-H-Si-Cl (MTS) system

Equilibrium gas phases				
C(g)	Si <sub>2</sub> (g)	C <sub>2</sub> Cl <sub>2</sub> (g)	C <sub>4</sub> (g)	SiCl <sub>3</sub> (g)
CCl(g)	CH <sub>2</sub> Cl <sub>2</sub> (g)	C <sub>2</sub> Cl <sub>4</sub> (g)	C <sub>5</sub> (g)	SiHCl <sub>3</sub> (g)
CCl <sub>2</sub> (g)	CH <sub>3</sub> (g)	C <sub>2</sub> Cl <sub>6</sub> (g)	Cl(g)	SiCl <sub>4</sub> (g)
CCl <sub>3</sub> (g)	CH <sub>3</sub> Cl(g)	C <sub>2</sub> H(g)	HCl(g)	H(g)
CCl <sub>4</sub> (g)	CH <sub>3</sub> SiCl <sub>3</sub> (g)	C <sub>2</sub> HCl(g)	SiH <sub>3</sub> Cl(g)	SiH(g)
CH(g)	CH <sub>4</sub> (g)	C <sub>2</sub> H <sub>2</sub> (g)	SiCl(g)	H <sub>2</sub> (g)
CHCl(g)	SiC(g)	C <sub>2</sub> H <sub>4</sub> (g)	SiCl <sub>2</sub> (g)	SiH <sub>4</sub> (g)
CHCl <sub>3</sub> (g)	Si <sub>2</sub> C(g)	SiC <sub>2</sub> (g)	Cl <sub>2</sub> (g)	Si(g)
CH <sub>2</sub> (g)	C <sub>2</sub> (g)	C <sub>3</sub> (g)	SiH <sub>2</sub> Cl <sub>2</sub> (g)	
Equilibrium condensed phases				
C[s]	Si[l]	Si[s]	α-SiC[s]	β-SiC[s]

Table 5. Species considered in the C-H-Si-Cl (CCl<sub>4</sub>, SiCl<sub>4</sub>) system

Equilibrium gas phases				
CCl(g)	C <sub>2</sub> H(g)	SiH <sub>3</sub> Cl(g)	SiCl <sub>3</sub> (g)	H <sub>2</sub> (g)
CCl <sub>4</sub> (g)	C <sub>2</sub> H <sub>2</sub> (g)	SiCl(g)	SiHCl <sub>3</sub> (g)	SiH <sub>4</sub> (g)
CH <sub>3</sub> (g)	C <sub>2</sub> H <sub>4</sub> (g)	SiCl <sub>2</sub> (g)	SiCl <sub>4</sub> (g)	Si(g)
CH <sub>3</sub> Cl(g)	Cl(g)	Cl <sub>2</sub> (g)	H(g)	
CH <sub>4</sub> (g)	HCl(g)	SiH <sub>2</sub> Cl <sub>2</sub> (g)	SiH(g)	
Equilibrium condensed phases				
C[s]	Si[l]	Si[s]	α-SiC[s]	β-SiC[s]

### (1) MTS/H<sub>2</sub>

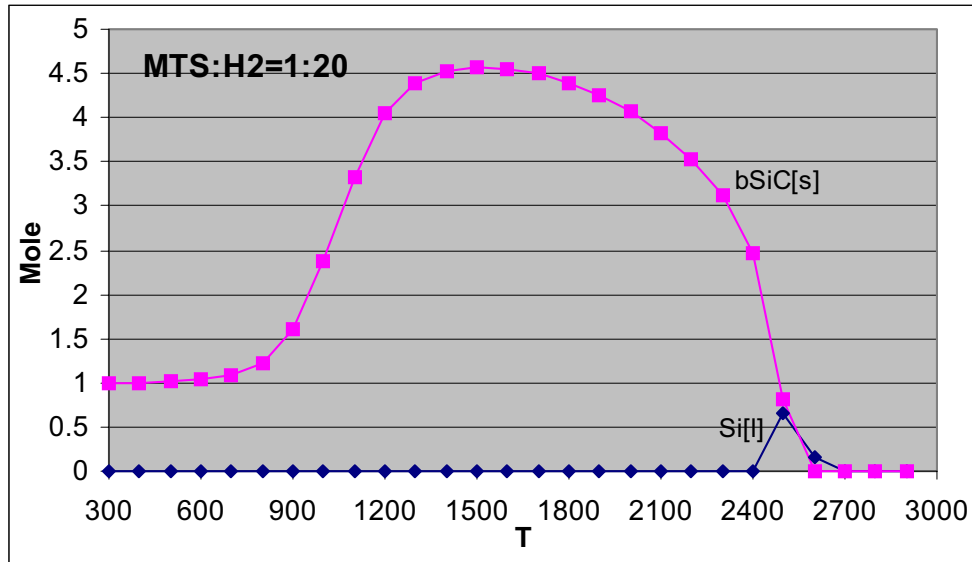
For the series of calculations based on MTS and hydrogen, the system was consistently defined with our experimental conditions. The moles of each element input were the values of actual moles in the reaction chamber multiplied by 1000. This adjustment was made because for some cases, the mole values were too small to get reasonable answers due to a quirk of the software. The pressure was kept as 500 Torr and the temperature ranged from 300 K to 2900 K. Three different ratios of hydrogen to MTS were used, which were 20, 60, and 100. The moles used to perform the calculations are listed in Table 6.

Table 6. Element input mole values

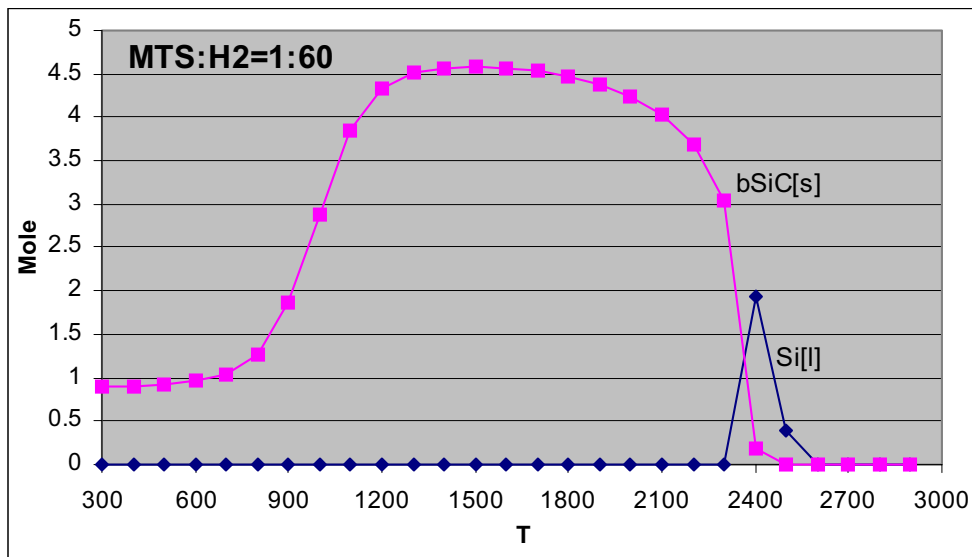
MTS: H <sub>2</sub>	C (mole)	H (mole)	Si (mole)	Cl (mole)
1:20	4.672	200.896	4.672	14.016
1:60	4.672	574.565	4.672	14.016
1:100	4.672	948.416	4.672	14.016

The calculated results of the condensed phases are shown in Figures 7(a) to 7(c). Because only β-SiC and liquid Si existed according to our calculations, the other condensed phases were not plotted here. In fact, according to the data of the JANAF Tables,<sup>10</sup> β-SiC is more stable than α-SiC. Therefore, no α-SiC was expected. From the Figures 7(a) to 7(c), it can be seen that under the indicated conditions, most of the time, β-SiC was the only condensed phase predicted to exist. The amount of β-SiC increased with temperature, reaching a maximum value, and then less β-SiC was predicted to form with increasing temperature. At higher temperatures, around 2400 K, the amount of β-SiC decreased dramatically and co-existed with liquid Si. The curves for β-SiC are similar in shape. Figure 8 shows the β-SiC curves for different MTS to H<sub>2</sub> ratios. Although it is not that pronounced, it is noted that at temperature less than 2300 K, more hydrogen helps to produce β-SiC; at temperatures greater than 2300 K, more hydrogen leads to less β-SiC. The curves show what would happen when the system is in equilibrium. There may be some deviations between the real SiC growth process and the predicted curves. However, these curves provide the tendency for producing β-SiC under different process conditions.

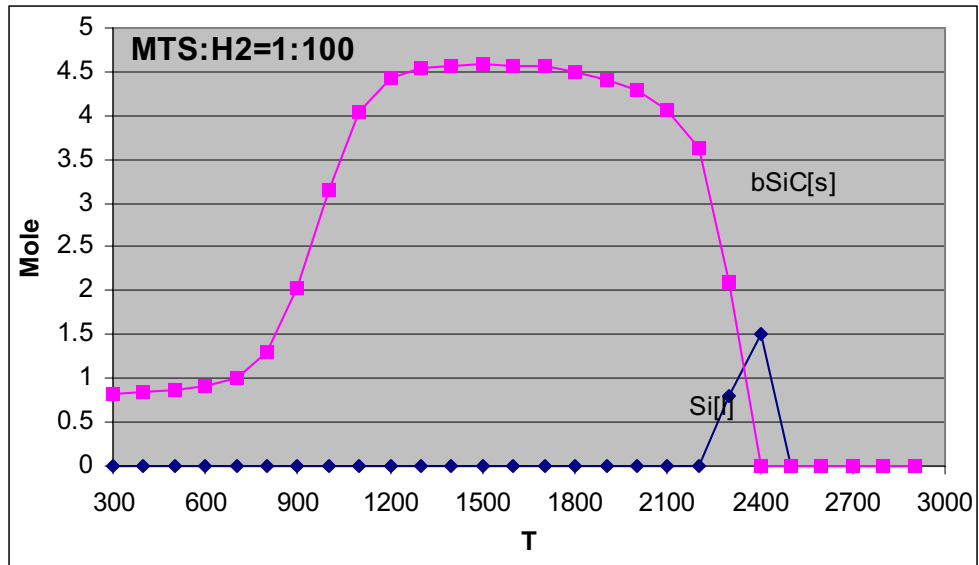
As mentioned before, the SiC fibers and lines grown using the Georgia Tech LVCD system had undesirable volcano effects.<sup>6</sup> From the previous calculations, in the temperature range of 1000 K to 2000 K, the amount of  $\beta$ -SiC increased with temperature and met the maximum value, then decreased with temperature (Figures 7 and 8). It is possible that these thermodynamic influences of the growth process are the reason for the volcano effects. To confirm this, further experiments and more modeling are required.



(a)



(b)



(c)

Figure 7 The condensed phases of system MTS/H<sub>2</sub> at pressure 500 Torr and MTS to H<sub>2</sub> ratios indicated

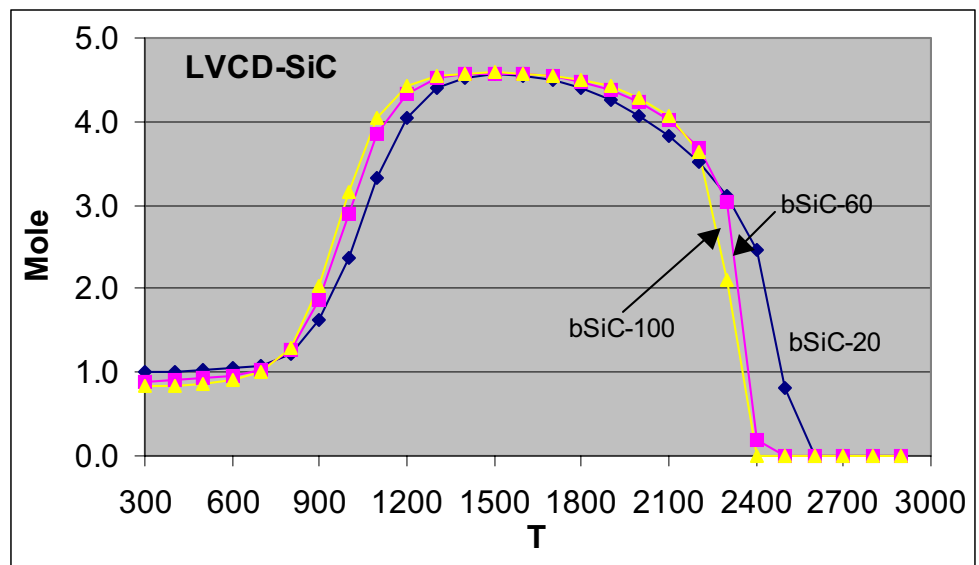


Figure 8  $\beta$ -SiC mole value curves at pressure of 500 Torr and MTS to H<sub>2</sub> ratios indicated

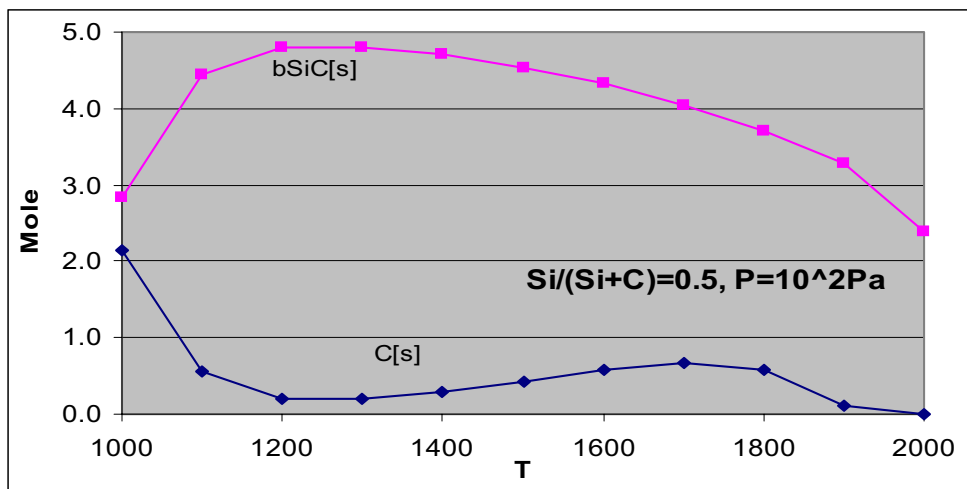
## (2) SiCl<sub>4</sub>/CCl<sub>4</sub>/H<sub>2</sub>

As previously mentioned, this series of calculations was performed as a check of the method by comparing with Kingon's results.<sup>9</sup> For a system of CCl<sub>4</sub>/SiCl<sub>4</sub>/H<sub>2</sub>, the total amount of Si and C was fixed as 10 moles, the ratio of H<sub>2</sub> to (Si+C) was 10, and the amount of Cl was 40 moles. The detailed information used to specify the calculations is shown in Table 7. For each set of calculations having a specific pressure and Si/ (Si+C)

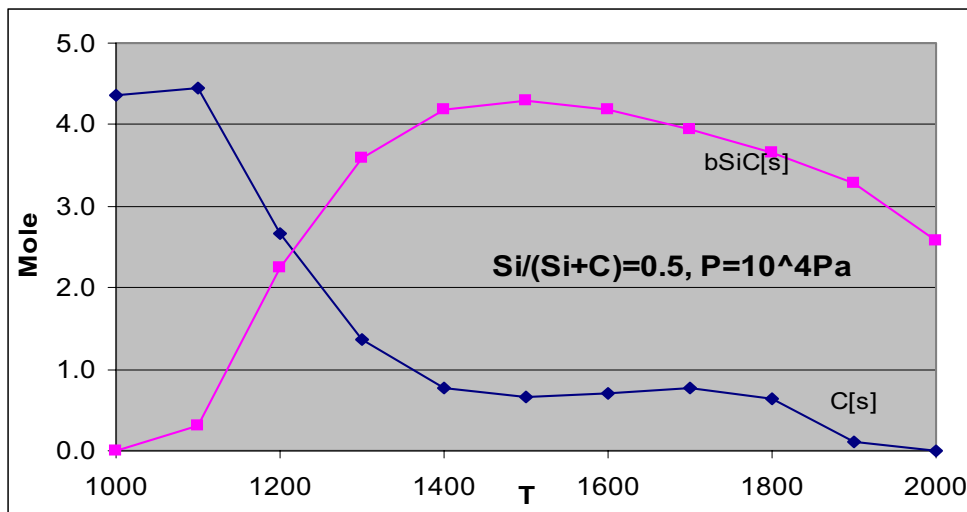
ratio, the temperature ranged from 1000 K to 2000 K. The calculated results are shown in Figure 9.

Table 7. Conditions used to specify the system of  $\text{CCl}_4/\text{SiCl}_4/\text{H}_2$

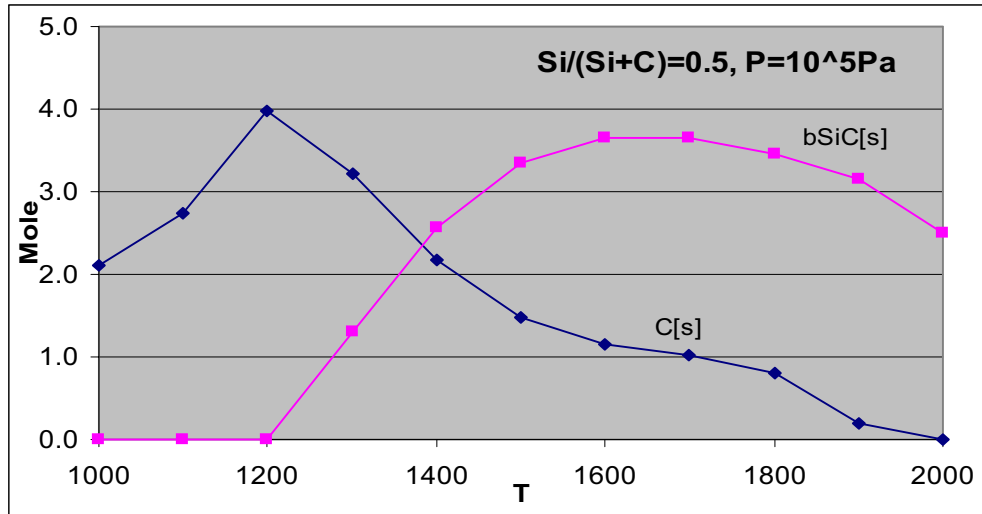
Pressure (Pa)	Si/(Si+C)				
$10^2$	0.1	0.3	0.5	0.7	0.9
$10^4$	0.1	0.3	0.5	0.7	0.9
$10^5$	0.1	0.3	0.5	0.7	0.9
$10^6$	0.1	0.3	0.5	0.7	0.9



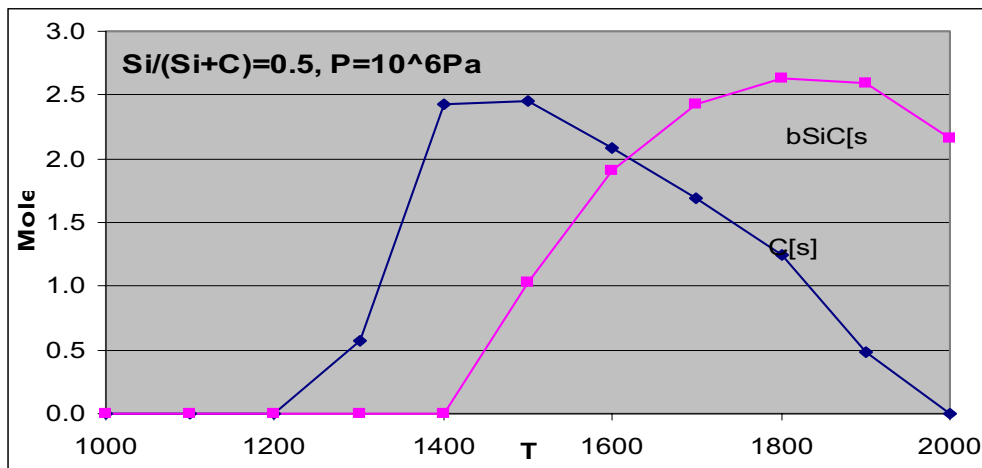
(a)



(b)



(c)



(d)

Figure 9 CCl<sub>4</sub>/SiCl<sub>4</sub>/H<sub>2</sub> system at Si/(Si+C)=0.5

In each case the calculations were in good agreement with Kingon's<sup>9</sup> results, which provide confidence for the MTS/H<sub>2</sub> calculations. Also, observing the relationship between the pressure and the amount of β-SiC, it seems that higher pressure inhibits the deposition of β-SiC. But there are no experimental data showing this relationship.

## Summary and Conclusions

LCVD-SiC fibers grown using the Georgia Tech LCVD system have surface structures that ranged from nodular, rounded columnar, strongly faceted, and needle like depending on the growth parameters. LCVD-SiC lines did not show any faceted surface structures. From our experiments, it can be concluded that the growth temperature, reactant concentration, and the substrate type play an important role in determining the morphology of LCVD-SiC.

Thermodynamic calculations on the system C-H-Si-Cl system using SOLGASMIX-PV software provide the basis for getting the most stable combination of condensed phases, especially to make  $\beta$ -SiC. The calculations suggest that the deposition rate increased with increasing temperature, reached a maximum, and then decreased. This information should be useful in establishing processing condition that permit the growth of uniform SiC fibers and lines that do not exhibit the volcano effect.

## Reference:

1. T. Noda, H. Suzuki, H. Araki, F. Abe, M. Okada, "Formation of polycrystalline SiC film by excimer-laser chemical vapour deposition", *Journal of Materials Science Letters* 11 p. 477-478, 1992.
2. J. Chin, P. K. Gantzel and R. G. Hudson, "The Structure of Chemical Vapor Deposition Silicon Carbide", *Thin Solid Films*, 40 p.57-72, 1977.
3. Byung Jin Choi, Dong Won Park, Dai Ryong Kim, "Chemical Vapour Deposition of Silicon Carbide by pyrolysis of methylchlorosilanes", *Journal of Materials Science Letters*, 16 p.33-36, 1997.
4. P. Tsui and K. E. Spear, "A Morphological Study of Silicon Carbide Prepared by Chemical Vapor Deposition", *Materials Science Research* 17 p. 371-80, 1984.
5. G. Eriksson, "Thermodynamic Studies of High temperature Equilibria," *Acta Chem. Scand.*, 25 [7] p. 2651-58, 1971.
6. D. Jean, C. Duty, R. Johnson, S. Bondi, and W. J. Lackey, "Carbon Fiber Growth Kinetics and Thermodynamics Using Temperature Controlled LCVD", *Carbon*, 40 (9) p. 1435-1445, 2002.
7. C. Duty, D. Jean, W. J. Lackey, "Design of a laser CVD rapid prototyping system", *Ceram. Eng. Sci. Proc.* 20 (4), p. 347-54, 1999.
8. K. A. Appiah, Z. L. Wang, W. J. Lackey, "Effects of deposition temperature on microstructure of laminated (SiC-C) matrix composites", *Journal of Materials Science* 35, p 1979-1984, 2000.
9. A. I. Kingon, L. J. Lutz, P. Liaw, and R. F. Davis, "Thermodynamic Calculation for the Chemical Vapor Deposition of Silicon Carbide," *J. Am. Ceram. Soc.*, 66 [8] p. 558-66, 1983.
10. JANAF Thermochemical Tables, 2<sup>nd</sup> ed., Natl. Stand. Ref. Data. Ser. (U. S. Natil. Bur. Stand.), No. 37, 1971